Microburst Scale Size Derived from Multiple Bounces of a Microburst Simultaneously Observed with the FIREBIRD-II CubeSats

Mykhaylo Shumko[1], John Sample[1], Arlo Johnson[1], Bern Blake[2], Alex Crew[3], Harlan Spence[4], David Klumpar[1], Oleksiy Agapitov[5], Matthew Handley[6]

[1]Department of Physics, Montana State University, Bozeman, Montana, USA
[2]Space Science Applications Laboratory, The Aerospace Corporation, Los Angeles, California, USA
[3]The Johns Hopkins University Applied Physics Laboratory LLC, Laurel, Maryland, USA
[4]Institute for the Study of Earth, Oceans, and Space, University of New Hampshire, Durham, New Hampshire, USA
[5]Space Sciences Laboratory, UC Berkeley, Berkeley, California, USA
[6]Los Alamos National Laboratory, Los Alamos, New Mexico, USA

Key Points:

- The lower bound lat/lon scale sizes of the microburst at LEO were 28.8 ± 0.8 km and 50.8 ± 11.4 km, respectively.
- Deduced lower bound equatorial scale size was similar to the whistler-mode chorus source scale.

Corresponding author: Mykhaylo Shumko, `msshumko@gmail.com`

Abstract

The FIREBIRD-II CubeSats simultaneously observed a spatially large microburst with multiple bounces on February 2nd, 2015 during a small storm. This is the first such microburst observed by two spacecraft, and we estimated its lower bound spatial scale sizes and bounce periods. Its lower bound latitudinal scale size was 28.8 ± 0.8 km and the longitudinal scale size was 50.8 ± 11.4 km in low earth orbit. We mapped these scale sizes to the magnetic equator and found that the radial and azimuthal scale sizes were at least 504 ± 14 km and 530 ± 119 km, respectively. These lower bound equatorial scale sizes are similar to whistler-mode chorus wave source scale sizes, which supports the hypothesis that microbursts are a product of electron scattering by chorus waves. **Next sentance still seems forced...** This unique observation coupled with FIREBIRD-II's high time and energy resolution allowed us to compare the observed electron bounce periods to four magnetic field models.

1 Introduction

The dynamics of radiation belt electrons are complex, and are driven by competition between source and loss processes. A few possible loss processes are radial diffusion [*Shprits and Thorne*, 2004], magnetopause shadowing [*Ukhorskiy et al.*, 2006], and pitch angle and energy diffusion due to scattering of electrons by plasma waves [e.g. *Abel and Thorne*, 1998; *Summers et al.*, 1998; *Meredith et al.*, 2002; *Selesnick et al.*, 2003; *Horne and Thorne*, 2003; *Thorne et al.*, 2005]. There are a variety of waves that cause pitch angle scattering, including electromagnetic ion cyclotron waves, plasmaspheric hiss, and chorus [*Millan and Thorne*, 2007; *Thorne*, 2010]. Chorus predominantly occurs in the dawn sector (6-12 magnetic local times (MLT))[*Li et al.*, 2009] where it accelerates electrons with large equatorial pitch angles and scatters electrons with small equatorial pitch angles [*Horne and Thorne*, 2003]. Some of these electrons may be impulsively scattered into the loss cone, where they result in short-duration (~ 100 ms) enhancements in precipitating flux called microbursts.

Anderson and Milton [1964] coined the term microburst to describe high altitude balloon observations of ~ 100 ms enhancements of bremsstrahlung X-rays emitted from scattered microburst electrons impacting the atmosphere. Since then, non-relativistic microbursts have routinely been observed with other balloon missions [*Parks*, 1967; *Woodger et al.*, 2015; *Anderson et al.*, 2017]. Interestingly, relativistic microbursts have not yet been observed by high altitude balloons in the dawn sector [*Millan et al.*, 2002; *Millan and Thorne*, 2007]. This may be due to relatively weaker pitch angle scattering of relativistic electrons by chorus [*Lee et al.*, 2012]. Microbursts have also been observed in low earth orbit (LEO) with, e.g. the SAMPEX > 150 keV and > 1 MeV channels [*Nakamura et al.*, 1995, 2000; *Blake et al.*, 1996; *Lorentzen et al.*, 2001a,b; *O'Brien et al.*, 2003, 2004; *Blum et al.*, 2015] and FIREBIRD-II with its > 200 keV energy channels [*Crew et al.*, 2016; *Anderson et al.*, 2017; *Breneman et al.*, 2017]. Microbursts and chorus waves predominantly occur in the dawn sector, are bursty [*Lorentzen et al.*, 2001b], and *Breneman et al.* [2017] made a direct observational link between microbursts and chorus.

Understanding microburst precipitation is important to radiation belt dynamics since they have been modeled and empirically estimated to deplete the relativistic electron population of the outer radiation belt on the order of a day [*O'Brien et al.*, 2004; *Thorne et al.*, 2005; *Shprits et al.*, 2007; *Breneman et al.*, 2017]. An important parameter in the estimation of instantaneous radiation belt electron losses due to microbursts is their scale size. *Parks* [1967] used balloon measurements of bremsstrahlung X-rays to estimate the scale size of predominantly low energy microbursts to be 40 ± 14 km. In *Blake et al.* [1996] a microburst with multiple bounces was observed by SAMPEX, and the microburst was estimated to have a latitudinal scale size of "at least a few tens of kilometers". *Blake et al.* [1996] concluded that typically microbursts are less than a few tens of electron gyroradii in size (at L = 5 at LEO, the gyroradii of 1 MeV electrons is on the order of 100 m). *Dietrich et al.* [2010] used

SAMPEX along with ground-based very low frequency stations to conclude that microbursts have scale sizes less than 4 km.

Since February 1st, 2015, microbursts have been observed by FIREBIRD-II, a pair of CubeSats in LEO. Soon after launch, when the two FIREBIRD-II spacecraft were at close range, a microburst with a scale size greater than 11 km was observed [*Crew et al.*, 2016]. On the same day, FIREBIRD-II simultaneously observed a microburst with multiple bounces. The microburst decay was observed over a period of a few seconds, while the spacecraft were traveling predominantly in latitude. Here we present the analysis and results of the latitude and longitude scale sizes of the first microburst with multiple bounces observed with two spacecraft.

The rest of this paper is organized as follows: in section 2, we introduce the spacecraft instrumentation and the microburst observation. In section 3, we describe the calculation of the microburst scale size in LEO and at the magnetic equator, as well as the electron bounce period. Lastly, in section 4, we compare the microburst scale size results to empirical estimates of chorus scale sizes.

2 Spacecraft and Observation

FIREBIRD-II is a pair of identically-instrumented 1.5U CubeSats (15 cm x 10 cm x 10 cm) that are designed to measure electron precipitation in LEO. The FIREBIRD-II CubeSats are identified as Flight Unit 3 (FU3) and Flight Unit 4 (FU4) and were launched on January 31st, 2015. Their orbit has a 632 km apogee, 433 km perigee, and 99° inclination [*Crew et al.*, 2016]. FU3 and FU4 are orbiting in a string of pearls configuration with FU4 ahead, to resolve the space-time ambiguity inherent to single spacecraft missions such as SAMPEX. Each FIREBIRD-II unit has a collimated and a surface solid state detector with complementary fields of view of 54° and 90°, respectively. They are observing electron fluxes in six energy channels from $\sim$ 230 keV to $>$ 1 MeV. Their adjustable sampling rate is 18.75 ms by default and can be at a fast as 12.5 ms.

On February 2nd, 2015 at 06:12:53 UT, during the transition between the main and recovery phases of a storm with a minimum Dst of -44 nT (Kp = 4, and AE $\approx$ 400 nT), a microburst and subsequent bounces were observed simultaneously on both spacecraft. Figure 1 shows the High Resolution (HiRes) microburst electron flux, sampled at 18.75 ms. Five peaks were observed on both spacecraft. FU3's collimated detector observed the microburst from the first energy channel (231 - 300 keV) to the fourth energy channel (555 - 771 keV), while on the surface detector it was observed up to the fifth energy channel (683 - 950 keV). Only FU3 has a functioning surface detector, so the rest of this analysis used the electron flux data from the collimated detectors, up to the fourth energy channel. Furthermore, since FU4's 5th peak in the fourth energy channel was comparable to the Poisson noise, only the first four peaks on FU4 were used in the spatial scale analysis.

The HiRes data in Fig. 1 shows signs of energy dispersion. With the aid of the black vertical bars in Fig. 1, the first peak does not appear to be dispersed, and subsequent peaks show dispersion consistent across energy channels. This dispersion signature and amplitude decay implies that the first peak was observed soon after the electrons were scattered, followed by decaying bounces.

At this time, FIREBIRD-II was at McIlwain L = 4.7 and MLT = 8.3, calculated with the Tsyganenko 1989 (T89) magnetic field model [*Tsyganenko*, 1989]. They were above Sweden, latitude = 63°N, longitude = 15°E, altitude = 650 km. At this location, any background electron flux that was in the drift loss cone was recently lost to the South Atlantic Anomaly, enabling FIREBIRD-II to make this unique observation. Outside of this region, the drift loss cone flux will quickly hide the returning bounces. Locally mirroring electrons would have mirrored at 95 km in the opposite hemisphere, calculated with T89 and IRBEM-Lib [*Boscher et al.*, 2012]. From the analysis done by *Fang et al.* [2010], the peak in the total ionization rate in the atmosphere for 100 keV electrons is around 80 km altitude, while 1 MeV electrons have a peak total ionization rate around 60 km altitude, so it is expected that a fraction of the microburst electrons will survive each encounter with the atmosphere. By plotting the peak flux as a function of bounce (not shown), it was found that 40 - 60 % of the microburst electrons were lost on the first bounce, similar to the 33% loss per bounce observed for a bouncing microburst observed by SAMPEX [*Thorne et al.*, 2005].

3 Analysis

At the beginning of the FIREBIRD-II mission, two issues prevented the proper analysis of the microburst's spatial scale size: the spacecraft clocks were not synchronized, and their relative positions were not accurately known. We addressed these issues with a cross-correlation time lag analysis described in detail in the supporting information. From this analysis, the time correction was 2.28 ± 0.12 s (applied to Fig. 1) and the separation was $d = 19.9 \pm 0.9$ km.

3.1 Microburst Scale Sizes

After we applied the corrections detailed in the supporting information, we mapped the locations of FU3 and FU4 in Fig. 2. The locations where FU3 saw peaks 1-5 and where FU4 saw peaks 1-4 are shown as P1-5 and P1-4, respectively. The lower bound on the latitudinal extent of the microburst was the difference in latitude between P1 on FU3 and P4 on FU4 and was found to be 28.8 ± 0.8 km. The uncertainty was estimated from the spacecraft separation uncertainty described in the supporting information. This scale size is the largest reported by FIREBIRD-II.

Need to reword the following sentence... To calculate the longitudinal scale size of the microburst, it is assumed that the scattered electrons observed in the last bounce by FIREBIRD-II, must have drifted from their initial scattering longitude, west of FIREBIRD-II's location. Following geometrical arguments, the distance that electrons drift azimuthally in a single bounce is a product of the circumference of the drift shell foot point, and the fraction of the total drift orbit traversed in a single bounce and is given by,

$$d_{az} = 2\pi(R_E + A)\cos(\lambda)\frac{t_b}{< T_d >} \tag{1}$$

where R_E is the Earth's radius, A is the spacecraft altitude, λ is the magnetic latitude, t_b is the electron bounce period, and $< T_d >$ is the electron drift period. *Parks* [2003] derived $< T_d >$ to be,

$$< T_d > \approx \begin{cases} 43.8/(L \cdot E) & \text{if } \alpha_0 = 90^\circ \\ 62.7/(L \cdot E) & \text{if } \alpha_0 = 0^\circ \end{cases} \tag{2}$$

where E is the electron energy in MeV, L is the L shell, and α_0 is the equatorial pitch angle. Electrons mirroring at FIREBIRD-II have $\alpha_0 \approx 3.7^\circ$ and so the $\alpha_0 = 0^\circ$ limit was used.

The microburst's longitudinal scale size is defined as the furthest distance that its electrons drifted east and were last seen. This was calculated with $D_{az} = n\, d_{az}$ where n is the number of bounces observed. The stars with energy labels in Fig. 2 represent the locations of electrons with that energy when the microburst was observed at P1, and drifted eastward to be last seen at P5 for FU3 and P4 for FU4. Using this methodology, the the larger longitudinal scale size was observed by FU3 and it was greater than 38.5 ± 8.8 km for the 555 keV electrons and greater than 50.8 ± 11.4 km for the 771 keV electrons, and is shown with the red dashed box in Fig. 2. The uncertainty was estimated by propagating the uncertainty in the spacecraft separation through Eq. 1.

The microburst's longitudinal and latitudinal scale sizes and their uncertainties at LEO were mapped to the magnetic equator with T89. The radial scale size (latitudinal scale mapped from LEO) was greater than 504 ± 14 km. The azimuthal scale size (longitudinal scale mapped from LEO) of 555 keV electrons was greater than 451 ± 103 km and for the 771 keV electrons it was greater than 530 ± 119 km.

3.2 Electron Bounce Period

We used this unique observation of bouncing electrons to calculate the bounce period, t_b as a function of energy and compare it to t_b derived from four magnetic field models. The observed t_b and uncertainties were calculated by fitting the baseline-subtracted HiRes flux. The baseline flux used in this analysis is given in *O'Brien et al.* [2004] as the flux at the 10th percentile over a specified time interval, which in this analysis was taken to be 0.5 seconds. The flux was fitted with a superposition of Gaussians for each energy channel, and the uncertainty in flux was calculated using the Poisson error from the microburst and baseline fluxes summed in quadrature. Using the fit parameters, the mean t_b for the lowest four energy channels is shown in Fig. 3 with green and purple rectangles. The trend of decreasing t_b as a function of energy is evident in Fig. 3. This energy dispersion signature further supports the assumption that the subsequent peaks are bounces, and not a train of microbursts scattered by bouncing chorus.

The bounces observed with FU3 had in-channel dispersion to earlier times in the lowest two energy channels (evident by the skewing of the observed peaks). This dispersion signature hints at the underlying electron flux spectra that is smeared out by the broad energy channels, and appears as skewing in the observed peaks. If FIREBIRD-II had finer energy resolution, the peak in the flux would be towards the higher energy end of the first energy channel. A Gaussian fit cannot account for this in-channel dispersion, and as a first order correction, minima between peaks was used to calculate t_b, and is shown in Fig. 3 with blue rectangles.

To compare the observed and modeled t_b, we superposed t_b curves for various models including an analytical solution in a dipole [*Schulz and Lanzerotti*, 1974], and numerical models: T89, Tsyganenko 2004 (T04) [*Tsyganenko and Sitnov*, 2005], and Olson & Pfitzer Quiet [*Olson and Pfitzer*, 1982] in Fig. 3. The numerical t_b curves were calculated using a Python wrapper for IRBEM-Lib. It traces the magnetic field line between mirror points, and calculates t_b assuming conservation of energy and the first adiabatic invariant for electrons mirroring at FIREBIRD-II. A discrepancy of $\approx$20% is present between the modeled and fit bounce periods in the lower energies, and is reduced at higher energies. The low energy discrepancy is removed by using the minima to calculate t_b for the < 555 keV peaks. Across all but one energy channel, the T04 model has the largest discrepancy compared to other models.

4 Discussion

The twin FIREBIRD-II CubeSats have enabled a direct estimate of the lower bound scale size of the large microburst studied here. This microburst was larger than the latitudinal scale sizes of > 1 MeV microbursts reported in *Blake et al.* [1996], was similar to the scale sizes of > 15 keV microbursts observed with a high altitude balloon [*Parks*, 1967] and was $\sim$ 10 times larger than reported in *Dietrich et al.* [2010]. Lastly, the microburst studied here was ~ 2.6 times larger than other simultaneous microbursts observed by FIREBIRD-II [*Crew et al.*, 2016]. No energy dependence on the scale size was observed.

The microburst scale size obtained in Section 3.1 and scaled to the geomagnetic equator can be compared with the scales of chorus waves presumably responsible for the rapid burst electron precipitation. Early direct estimates of the chorus source scales were made by the coordinated measurement by ISEE-1, 2. The wave power correlation scale was estimated to be about several hundred kilometers across the background magnetic field [*Gurnett et al.*, 1979]. *Santolik et al.* [2003] determined the correlation lengths of chorus-type whistler waves to be around 100 km based on multipoint CLUSTER Wide Band Data measurements near the chorus source region during the magnetic storm of 18 April 2002 at L shell about 4. *Agapitov et al.* [2010, 2011, 2017] recently showed that the spatial extent of chorus source region can be larger: from 600 km in the outer radiation belt to more than 1000 km in the outer magnetosphere. The lower bound azimuthal and latitudinal scales obtained in Section 3.1 and scaled to the magnetic equator, are similar to the whistler-mode chorus source scale sizes reported in *Agapitov et al.* [2011, 2017].

No wave measurements from nearby spacecraft were available at this time. Nevertheless, during the hours before and after this observation, the Van Allen Probes' [*Mauk et al.*, 2013] Electric and Magnetic Field Instrument and Integrated Science [*Kletzing et al.*, 2013] observed strong wave power in the lower band chorus frequency range, inside the outer radiation belt between 22 and 2 MLT. Furthermore, AE $\sim$ 400 nT at this time, and relatively strong chorus waves were statistically more likely to be present at FIREBIRD-II's MLT [*Li et al.*, 2009]. With the evidence presented, we conclude that the microburst electrons were likely scattered by chorus, similar to the conclusions made by e.g. *Lorentzen et al.* [2001a]; *O'Brien et al.* [2003]; *Breneman et al.* [2017].

The empirically estimated and modeled t_b in this study agree within FIREBIRD-II's uncertainties. This agreement implies that the real and modeled magnetic field line lengths are comparable. This is expected since the magnetoshere is not drastically compressed at 8 MLT, but we expect a larger discrepancy near midnight, where the magnetosphere is more stretched. This analysis can be used as a diagnostic tool for validating field line lengths in future studies.

This paragraph seems out of place... Lastly, we investigated the energy spectra of this microburst. Using the fit parameters from section 3.2, we calculated the exponential E-folding energy, $E_0 \sim 100\ keV$. This is similar to the results in *Lee et al.* [2005] who used STSAT-1 and *Datta et al.* [1997] who used a sounding rocket. It is soft for a typical microburst observed with FIREBIRD-II. There was no statistically significant change in E_0 for subsequent bounces.

5 Conclusions

This was a first observation of a large microburst with multiple bounces made possible by the twin FIREBIRD-II CubeSats. Its lower bound LEO latitudinal and longitudinal scale sizes of 28.8 ± 0.8 km and 50.8 ± 11.4 km make it one of the largest observed. No energy dependence on the scale size was observed. Furthermore, its lower bound LEO scale sizes mapped to the magnetic equator were 504 ± 14 km radially and 530 ± 119 km azimuthally. The bounce periods calculated with the Gaussian fit and minima methods are in good agreement with the numerically estimated bounce periods, confirming that the energy-dependent dispersion was due to bouncing. The similarity of the microburst and chorus source region scale sizes, as well as magnetospheric location and condition, further support the correlation between microbursts and chorus.

Acknowledgments
This work was made possible with help from the FIREBIRD team, and the members of the Space Sciences and Engineering Laboratory at Montana State University for their hard work to make this mission a success. In addition, I acknowledge Drew Turner for his suggestions regarding the bounce period calculations. The FIREBIRD-II data are available at http://solar.physics.montana.edu/FIREBIRD_II/. This material is based upon work at Montana State University supported by the National Science Foundation under Grant Numbers 0838034 and 1339414.

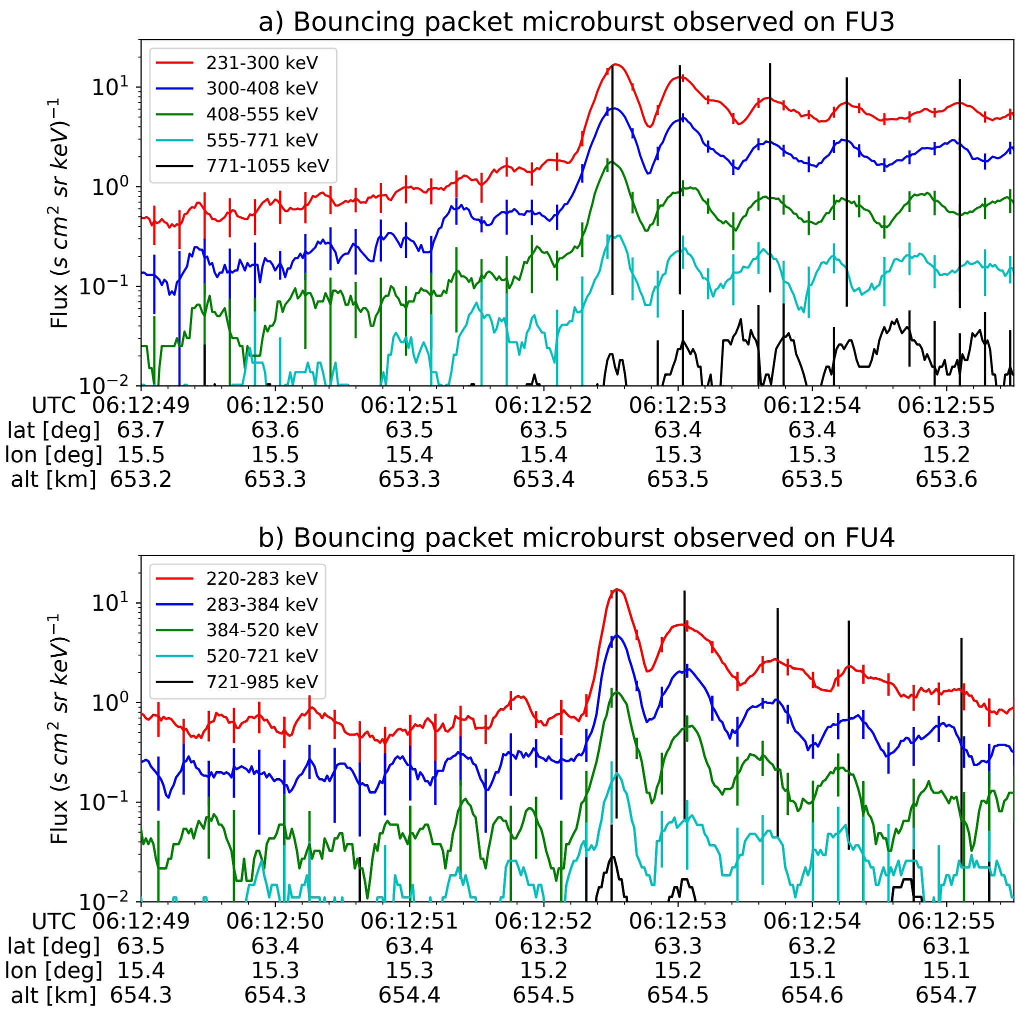

Figure 1. HiRes data of the microburst observed at February 2nd, 2015 at 06:12:53 UT, smoothed with a 150 ms rolling average. The subsequent bounces showed some energy dispersion. As discussed in the supporting information, a time correction of -2.28 s was applied to FU3. While the flux from five energy channels is shown, only channels with reasonable counting statistics were used for the spatial scale analysis. Vertical colored bars show the $\sqrt{N}$ error every 10th data point and vertical black bars are lined up with the peaks in the 220-283 keV energy channel to help identify dispersion.

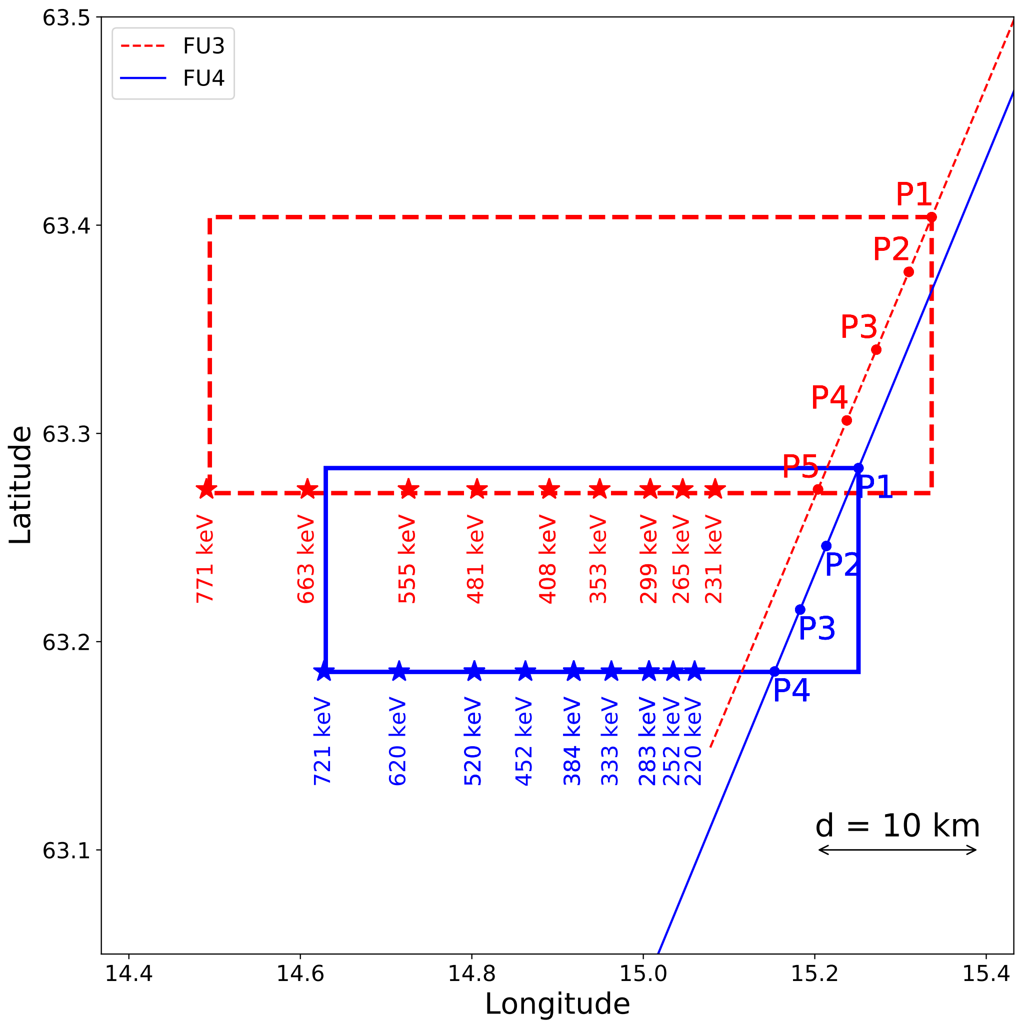

Figure 2. The topology of the FIREBIRD-II orbit and the multiple bounces of the microburst projected onto latitude and longitude with axis scaled to equal distance. Attributes relating to FU3 shown in red dashed lines, and FU4 with blue solid lines. The spacecraft path is shown with the diagonal lines, starting at the upper right corner. The labels P1-4 for FU4 and P1-5 for FU3 indicate where the spacecraft were when the Nth peak was seen in the lowest energy channel in the HiRes data. The stars with the accompanying energy labels represent the locations of the electrons with that energy that started at time of P1, and were seen at the last peak on each spacecraft. The rectangles represent the lower bound of the microburst scale size, assuming that the majority of the electrons were in the upper boundary of energy channel 4.

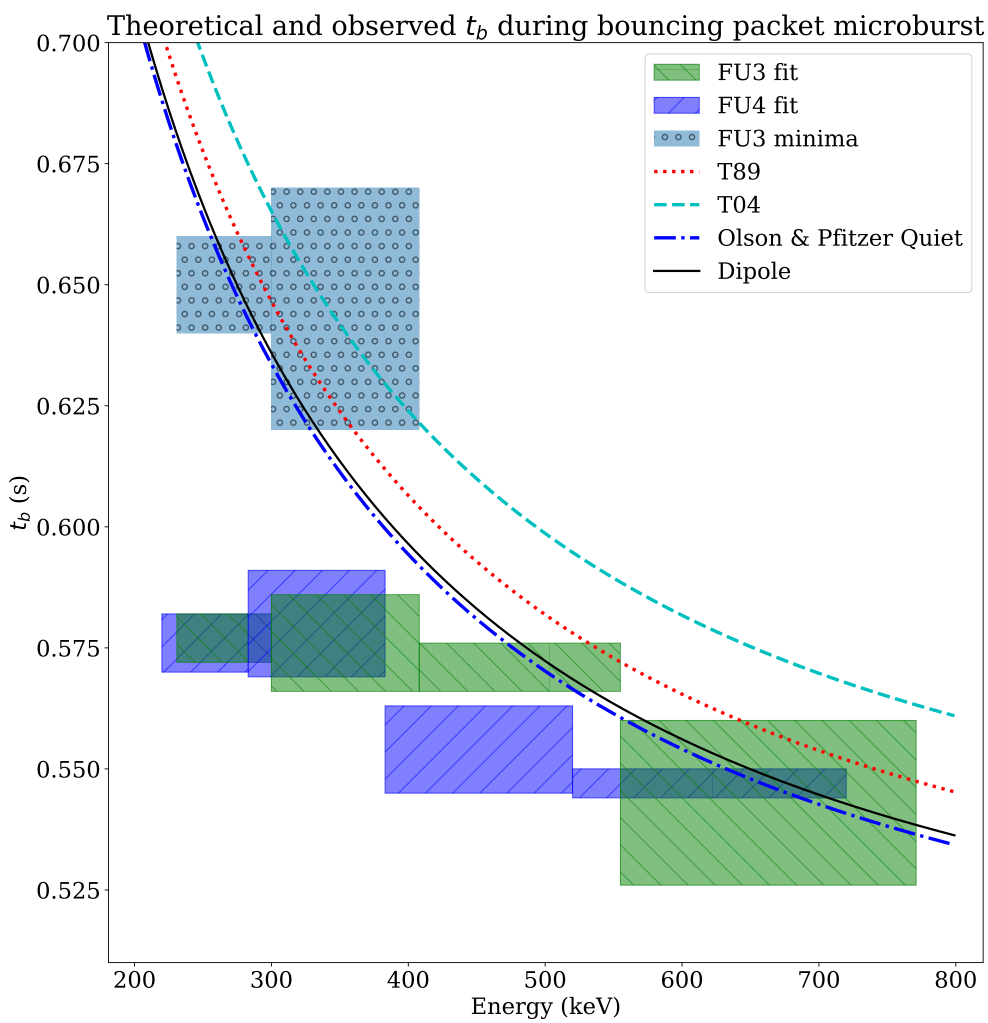

Figure 3. Observed and theoretical t_b for electrons of energies from 200 to 770 keV. The solid black line is t_b in a dipole magnetic field, derived in *Schulz and Lanzerotti* [1974]. The red and cyan dashed lines are the t_b derived using the T89, and T04 magnetic field models with IRBEM. Lastly, the blue dashed curve is the t_b derived using the Olson & Pfitzer Quiet model. The green and purple rectangles represent the observed t_b for FU3 and FU4 using a Gaussian fit, respectively. The blue rectangles represent the observed t_b calculated with the minima between the bounces. The width of the boxes represent the width of those energy channels, and the height represents the uncertainty from the fit.

References

Abel, B., and R. M. Thorne (1998), Electron scattering loss in earth's inner magnetosphere: 1. dominant physical processes, *Journal of Geophysical Research: Space Physics*, *103*(A2), 2385–2396.

Agapitov, O., V. Krasnoselskikh, Y. Zaliznyak, V. Angelopoulos, O. Le Contel, and G. Rolland (2010), Chorus source region localization in the earth's outer magnetosphere using themis measurements, *Annales Geophysicae*, *28*(6), 1377–1386, doi:10.5194/angeo-28-1377-2010.

Agapitov, O., V. Krasnoselskikh, T. Dudok de Wit, Y. Khotyaintsev, J. S. Pickett, O. Santolik, and G. Rolland (2011), Multispacecraft observations of chorus emissions as a tool for the plasma density fluctuations' remote sensing, *Journal of Geophysical Research: Space Physics*, *116*(A9), n/a–n/a, doi:10.1029/2011JA016540, a09222.

Agapitov, O., L. W. Blum, F. S. Mozer, J. W. Bonnell, and J. Wygant (2017), Chorus whistler wave source scales as determined from multipoint van allen probe measurements, *Geophysical Research Letters*, pp. n/a–n/a, doi:10.1002/2017GL072701, 2017GL072701.

Anderson, B., S. Shekhar, R. Millan, A. Crew, H. Spence, D. Klumpar, J. Blake, T. O'Brien, and D. Turner (2017), Spatial scale and duration of one microburst region on 13 august 2015, *Journal of Geophysical Research: Space Physics*.

Anderson, K. A., and D. W. Milton (1964), Balloon observations of x rays in the auroral zone: 3. high time resolution studies, *Journal of Geophysical Research*, *69*(21), 4457–4479, doi:10.1029/JZ069i021p04457.

Blake, J., M. Looper, D. Baker, R. Nakamura, B. Klecker, and D. Hovestadt (1996), New high temporal and spatial resolution measurements by sampex of the precipitation of relativistic electrons, *Advances in Space Research*, *18*(8), 171 – 186, doi: http://dx.doi.org/10.1016/0273-1177(95)00969-8.

Blum, L., X. Li, and M. Denton (2015), Rapid mev electron precipitation as observed by sampex/hilt during high-speed stream-driven storms, *Journal of Geophysical Research: Space Physics*, *120*(5), 3783–3794, doi:10.1002/2014JA020633, 2014JA020633.

Boscher, D., S. Bourdarie, P. O'Brien, T. Guild, and M. Shumko (2012), Irbem-lib library.

Breneman, A., A. Crew, J. Sample, D. Klumpar, A. Johnson, O. Agapitov, M. Shumko, D. Turner, O. Santolik, J. Wygant, et al. (2017), Observations directly linking relativistic electron microbursts to whistler mode chorus: Van allen probes and firebird ii, *Geophysical Research Letters*.

Crew, A. B., H. E. Spence, J. B. Blake, D. M. Klumpar, B. A. Larsen, T. P. O'Brien, S. Driscoll, M. Handley, J. Legere, S. Longworth, K. Mashburn, E. Mosleh, N. Ryhajlo, S. Smith, L. Springer, and M. Widholm (2016), First multipoint in situ observations of electron microbursts: Initial results from the nsf firebird ii mission, *Journal of Geophysical Research: Space Physics*, *121*(6), 5272–5283, doi:10.1002/2016JA022485, 2016JA022485.

Datta, S., R. Skoug, M. McCarthy, and G. Parks (1997), Modeling of microburst electron precipitation using pitch angle diffusion theory, *Journal of Geophysical Research: Space Physics*, *102*(A8), 17,325–17,333.

Dietrich, S., C. J. Rodger, M. A. Clilverd, J. Bortnik, and T. Raita (2010), Relativistic microburst storm characteristics: Combined satellite and ground-based observations, *Journal of Geophysical Research: Space Physics*, *115*(A12).

Fang, X., C. E. Randall, D. Lummerzheim, W. Wang, G. Lu, S. C. Solomon, and R. A. Frahm (2010), Parameterization of monoenergetic electron impact ionization, *Geophysical Research Letters*, *37*(22).

Gurnett, D., R. Anderson, F. Scarf, R. Fredricks, and E. Smith (1979), Initial results from the isee-1 and-2 plasma wave investigation, *Space Science Reviews*, *23*(1), 103–122.

Horne, R. B., and R. M. Thorne (2003), Relativistic electron acceleration and precipitation during resonant interactions with whistler-mode chorus, *Geophysical Research Letters*, *30*(10), n/a–n/a, doi:10.1029/2003GL016973, 1527.

Kletzing, C., W. Kurth, M. Acuna, R. MacDowall, R. Torbert, T. Averkamp, D. Bodet, S. Bounds, M. Chutter, J. Connerney, et al. (2013), The electric and magnetic field instrument suite and integrated science (emfisis) on rbsp, *Space Science Reviews*, *179*(1-4), 127–181.

Lee, J.-J., G. K. Parks, K. W. Min, H. J. Kim, J. Park, J. Hwang, M. P. McCarthy, E. Lee, K. S. Ryu, J. T. Lim, E. S. Sim, H. W. Lee, K. I. Kang, and H. Y. Park (2005), Energy spectra of 170-360 kev electron microbursts measured by the korean stsat-1, *Geophysical Research Letters*, *32*(13), doi:10.1029/2005GL022996, l13106.

Lee, J. J., G. K. Parks, E. Lee, B. T. Tsurutani, J. Hwang, K. S. Cho, K.-H. Kim, Y. D. Park, K. W. Min, and M. P. McCarthy (2012), Anisotropic pitch angle distribution of 100 kev microburst electrons in the loss cone: measurements from stsat-1, *Annales Geophysicae*, *30*(11), 1567–1573, doi:10.5194/angeo-30-1567-2012.

Li, W., R. M. Thorne, V. Angelopoulos, J. Bortnik, C. M. Cully, B. Ni, O. LeContel, A. Roux, U. Auster, and W. Magnes (2009), Global distribution of whistler-mode chorus waves observed on the themis spacecraft, *Geophysical Research Letters*, *36*(9), n/a–n/a, doi:10.1029/2009GL037595, l09104.

Lorentzen, K. R., J. B. Blake, U. S. Inan, and J. Bortnik (2001a), Observations of relativistic electron microbursts in association with vlf chorus, *Journal of Geophysical Research: Space Physics*, *106*(A4), 6017–6027, doi:10.1029/2000JA003018.

Lorentzen, K. R., M. D. Looper, and J. B. Blake (2001b), Relativistic electron microbursts during the gem storms, *Geophysical Research Letters*, *28*(13), 2573–2576, doi:10.1029/2001GL012926.

Mauk, B., N. J. Fox, S. Kanekal, R. Kessel, D. Sibeck, and A. Ukhorskiy (2013), Science objectives and rationale for the radiation belt storm probes mission, *Space Science Reviews*, *179*(1-4), 3–27.

Meredith, N., R. Horne, D. Summers, R. Thorne, R. Iles, D. Heynderickx, and R. Anderson (2002), Evidence for acceleration of outer zone electrons to relativistic energies by whistler mode chorus, in *Annales Geophysicae*, vol. 20, pp. 967–979.

Millan, R., and R. Thorne (2007), Review of radiation belt relativistic electron losses, *Journal of Atmospheric and Solar-Terrestrial Physics*, *69*(3), 362 – 377, doi: http://dx.doi.org/10.1016/j.jastp.2006.06.019, global Aspects of Magnetosphere-Ionosphere CouplingGlobal Aspects of Magnetosphere-Ionosphere Coupling.

Millan, R. M., R. Lin, D. Smith, K. Lorentzen, and M. McCarthy (2002), X-ray observations of mev electron precipitation with a balloon-borne germanium spectrometer, *Geophysical research letters*, *29*(24).

Nakamura, R., D. N. Baker, J. B. Blake, S. Kanekal, B. Klecker, and D. Hovestadt (1995), Relativistic electron precipitation enhancements near the outer edge of the radiation belt, *Geophysical Research Letters*, *22*(9), 1129–1132, doi:10.1029/95GL00378.

Nakamura, R., M. Isowa, Y. Kamide, D. Baker, J. Blake, and M. Looper (2000), Observations of relativistic electron microbursts in association with vlf chorus, *J. Geophys. Res*, *105*, 15,875–15,885.

O'Brien, T. P., K. R. Lorentzen, I. R. Mann, N. P. Meredith, J. B. Blake, J. F. Fennell, M. D. Looper, D. K. Milling, and R. R. Anderson (2003), Energization of relativistic electrons in the presence of ulf power and mev microbursts: Evidence for dual ulf and vlf acceleration, *Journal of Geophysical Research: Space Physics*, *108*(A8), n/a–n/a, doi:10.1029/2002JA009784, 1329.

O'Brien, T. P., M. D. Looper, and J. B. Blake (2004), Quantification of relativistic electron microburst losses during the gem storms, *Geophysical Research Letters*, *31*(4), n/a–n/a, doi:10.1029/2003GL018621, l04802.

Olson, W. P., and K. A. Pfitzer (1982), A dynamic model of the magnetospheric magnetic and electric fields for july 29, 1977, *Journal of Geophysical Research: Space Physics*, *87*(A8), 5943–5948, doi:10.1029/JA087iA08p05943.

Parks, G. (2003), *Physics Of Space Plasmas: An Introduction, Second Edition*, Westview Press.

Parks, G. K. (1967), Spatial characteristics of auroral-zone x-ray microbursts, *Journal of Geophysical Research*, *72*(1), 215–226.

Santolik, O., D. Gurnett, J. Pickett, M. Parrot, and N. Cornilleau-Wehrlin (2003), Spatio-temporal structure of storm-time chorus, *Journal of Geophysical Research: Space Physics*, *108*(A7).

Schulz, M., and L. J. Lanzerotti (1974), *Particle Diffusion in the Radiation Belts*, Springer.

Selesnick, R. S., J. B. Blake, and R. A. Mewaldt (2003), Atmospheric losses of radiation belt electrons, *Journal of Geophysical Research: Space Physics*, *108*(A12), doi: 10.1029/2003JA010160, 1468.

Shprits, Y. Y., and R. M. Thorne (2004), Time dependent radial diffusion modeling of relativistic electrons with realistic loss rates, *Geophysical Research Letters*, *31*(8), n/a–n/a, doi:10.1029/2004GL019591, l08805.

Shprits, Y. Y., N. P. Meredith, and R. M. Thorne (2007), Parameterization of radiation belt electron loss timescales due to interactions with chorus waves, *Geophysical Research Letters*, *34*(11), n/a–n/a, doi:10.1029/2006GL029050, l11110.

Summers, D., R. M. Thorne, and F. Xiao (1998), Relativistic theory of wave-particle resonant diffusion with application to electron acceleration in the magnetosphere, *Journal of Geophysical Research: Space Physics*, *103*(A9), 20,487–20,500.

Thorne, R. M. (2010), Radiation belt dynamics: The importance of wave-particle interactions, *Geophysical Research Letters*, *37*(22), doi:10.1029/2010GL044990, l22107.

Thorne, R. M., T. P. O'Brien, Y. Y. Shprits, D. Summers, and R. B. Horne (2005), Timescale for mev electron microburst loss during geomagnetic storms, *Journal of Geophysical Research: Space Physics*, *110*(A9), n/a–n/a, doi:10.1029/2004JA010882, a09202.

Tsyganenko, N. (1989), A solution of the chapman-ferraro problem for an ellipsoidal magnetopause, *Planetary and Space Science*, *37*(9), 1037 – 1046, doi: http://dx.doi.org/10.1016/0032-0633(89)90076-7.

Tsyganenko, N. A., and M. I. Sitnov (2005), Modeling the dynamics of the inner magnetosphere during strong geomagnetic storms, *Journal of Geophysical Research: Space Physics*, *110*(A3), n/a–n/a, doi:10.1029/2004JA010798, a03208.

Ukhorskiy, A. Y., B. J. Anderson, P. C. Brandt, and N. A. Tsyganenko (2006), Storm time evolution of the outer radiation belt: Transport and losses, *Journal of Geophysical Research: Space Physics*, *111*(A11), n/a–n/a, doi:10.1029/2006JA011690, a11S03.

Woodger, L., A. Halford, R. Millan, M. McCarthy, D. Smith, G. Bowers, J. Sample, B. Anderson, and X. Liang (2015), A summary of the barrel campaigns: Technique for studying electron precipitation, *Journal of Geophysical Research: Space Physics*, *120*(6), 4922–4935.